Photocatalytic conversion of methane

Leny Yuliati† and Hisao Yoshida*

Received 9th April 2008
First published as an Advance Article on the web 16th June 2008
DOI: 10.1039/b710575b

Various efforts have been carried out to convert methane to more useful chemicals and hydrogen. However, due to its high stability, high energy is usually consumed for its conversion, which still remains as a problem to be solved. Recently, photocatalysis has been proposed to be one of the answers to break the thermodynamic barrier. This *tutorial review* provides a brief history about developments in the methane conversion and specially highlights the developments in the photocatalytic conversion of methane, such as methane coupling and methane conversion with other molecules.

1. Introduction

1.1 Importance of the methane utilization

Since methane is one of the most stable molecules, it can be abundantly found underground and on the surface. Methane is the major component (70–90%) of natural gas, which is nearly ubiquitous in the world. The natural gas can be found profusely not only in the conventional gas fields but also in many places such as deep underground and coal seam. In addition, recently, methane hydrate was discovered, in which methane molecules exist in a lattice of frozen water. On the other hand, besides these kinds of methane as an underground resource or fossil fuel, methane is also naturally generated from biosystems and can be produced artificially from biomass by biotechnology or biomass technology, which is renewable methane.

Department of Applied Chemistry, Graduate School of Engineering, Nagoya University, Furo-cho, Chikusa-ku, Nagoya, 464-8603, Japan. E-mail: yoshidah@apchem.nagoya-u.ac.jp
† Present address: Department of Chemical System Engineering, The University of Tokyo, 7-3-1 Hongo, Bunkyo-ku, Tokyo 113-8656, Japan

Since methane is a clean fuel among other conventional fuels and can be transported *via* pipes easily, methane is conveniently used as a fuel by a direct burning with oxygen or a catalytic combustion (Table 1, Entry 4) to obtain the heat energy (ΔH^0 (298 K) = −802 kJ mol^{-1}). However, we must keep in mind that methane is an important carbon source. Thus, methane should be used as not only a fuel but also a chemical source. Further development of technology for methane conversion to more useful carbon chemicals is highly desired. On the other hand, nowadays hydrogen is expected as a cleaner fuel. Methane has attracted much attention as a good hydrogen source since it has the highest H/C ratio among the hydrocarbons. Moreover, methane is recognized as one of the greenhouse gases with a higher global warming potential (GWP) than that of CO_2. When averaged over 100 years, methane warms the earth 25 times as much as the same mass of CO_2.[1] These facts mentioned above have made the utilization of methane one of the most desired issues today.

1.2 Methane conversion from thermodynamic view

Methane is a symmetrical molecule and a very stable hydrocarbon. As listed in Table 2, the energy to break the C–H bond is 434 kJ mol^{-1}, which is higher than those for C–H and C–C

Leny Yuliati

Leny Yuliati received a degree in chemistry from Gadjah Mada University in 2000. She received her degrees of M. Eng (2005) and PhD (2008) from Nagoya University. Presently, she is joining the group of Prof. Kazunari Domen at the University of Tokyo as a JSPS postdoctoral researcher. Her current research focuses on heterogeneous photocatalysis, especially for methane activation.

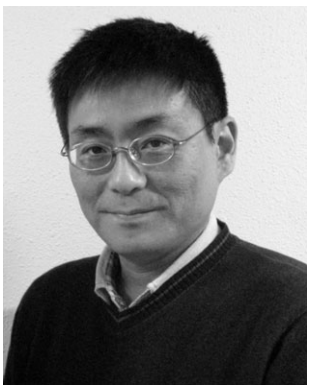

Hisao Yoshida

Hisao Yoshida received his degrees of B. Eng. (1991), M. Eng. (1993) and PhD (1998) from Kyoto University. He works at Nagoya University, where he has been a research associate from 1995 and an associate professor from 2003 to the present. His current research focuses on heterogeneous photocatalysis, especially for methane activation, hydrogen production and novel organic synthesis. He received the Catalysis Congress Prize of the International Association of Catalysis Societies in 2000 and the Prize for Young Scientists of Catalysis Society of Japan in 2003.

Table 1 Change of Gibbs free energy for various reactions

Entry	Reactions	Chemical equations	ΔG^0 (298 K)/kJ mol^{-1}
(1) *Methane only*			
1	Pyrolysis	$CH_4 \rightarrow C + 2H_2$	50.7
2	Non-oxidative coupling of methane (NOCM)	$2CH_4 \rightarrow C_2H_6 + H_2$	68.6
3	Aromatization	$6CH_4 \rightarrow C_6H_6 + 9H_2$	434
(2) *Methane and oxygen*			
4	Total oxidation	$CH_4 + 2O_2 \rightarrow CO_2 + 2H_2O$	−801
5	Oxidative coupling of methane (OCM)	$4CH_4 + O_2 \rightarrow 2C_2H_6 + 2H_2O$	−320
		$2CH_4 + O_2 \rightarrow C_2H_4 + 2H_2O$	−288
6	Partial oxidation of methane (POM)	$2CH_4 + O_2 \rightarrow 2CH_3OH$	−223
7	POM	$2CH_4 + O_2 \rightarrow 2CO + 4H_2$	−173
8	POM	$2CH_4 + O_2 \rightarrow 2HCHO + 2H_2$	−104
(3) *Methane and water*			
9	Methane to methanol	$CH_4 + H_2O \rightarrow CH_3OH + H_2$	117
10	Steam reforming of methane (SRM)	$CH_4 + H_2O \rightarrow CO + 3H_2$	142
11	Water–gas shift reaction	$CO + H_2O \rightarrow CO_2 + H_2$	−28.6
12	SRM + water–gas shift reaction	$CH_4 + 2H_2O \rightarrow CO_2 + 4H_2$	114
(4) *Methane and carbon dioxide*			
13	Methane to acetic acid	$CH_4 + CO_2 \rightarrow CH_3COOH$	71.1
14	Methane to acetone	$2CH_4 + CO_2 \rightarrow CH_3COCH_3 + H_2O$	115
15	CO_2 (dry) reforming of methane (DRM)	$CH_4 + CO_2 \rightarrow 2CO + 2H_2$	171
(5) *Methane and aqueous ammonia*			
16	Methane to amino acids	$2CH_4 + NH_3 + 2H_2O \rightarrow H_2NCH_2COOH + 5H_2$	204

bonds in higher hydrocarbons such as ethane, though it is lower than that for a C–H bond in benzene. Methane has no functional group and no polar distribution to facilitate chemical interactions, resulting in a low chemical reactivity. High photoenergy in the vacuum ultraviolet (VUV) region is required to excite methane *via* electronic transition, *i.e.*, the electronic absorption band of methane lies at a wavelength shorter than 140 nm.[2] To ionize methane, $CH_4 + h\nu \rightarrow CH_4^+ + e^-$, higher energy is necessary such as 12.6 eV, which corresponds to 98.3 nm of VUV light.

In the thermodynamic view, a reaction can proceed preferably when the change of the Gibbs free energy (ΔG) is negative and enough activation energy is given. This ΔG could be easily estimated by subtracting the sum of each Gibbs free energy of formation (ΔG_f^0) of the reactants from that of the products. The ΔG_f^0 for some molecules are shown in Table 3. For example, methane has more negative value of ΔG_f^0 than ethane and hydrogen. Thus, the ΔG^0 for non-oxidative coupling of methane (NOCM) is positive (Table 1, Entry 2), meaning that the reaction is thermodynamically unfavorable. We can also calculate the equilibrium constant, K, from this ΔG^0 as shown in eqn (1),

$$\Delta G^0(T) = -RT\ln K, \quad (1)$$

where T = temperature and R = gas constant. The composition of products in the equilibrium then can be estimated when the composition of the initial reactants is given. For example, in the case of NOCM, K is *ca.* 9.5×10^{-13} and the ethane yield is *ca.* 0.0002% in the equilibrium at 298 K. This shows that the NOCM hardly occurs at atmospheric pressure and room temperature.

Most of methane conversions are thermodynamically unfavorable at 298 K due to the positive and large value of the ΔG^0 (Table 1, Entries 1–3, 9–10, 12–16), except for methane activation with oxygen (Table 1, Entries 4–8). Thus, a high reaction temperature is basically required for them. In order to promote such reactions, not only enough energy but also suitable catalysts reducing the activation energy are very important. Moreover, it should be noted here that the actual reactivity of methane could not be estimated only from the thermodynamic property of the reaction since it would be greatly affected by the properties of the catalyst employed.

The values of Gibbs free energy of formation, ΔG_f^0, for some hydrocarbons as a function of temperature are shown in Fig. 1,[3] where the values per carbon number ($\Delta G_{f/c}^0$) are plotted for the sake of simplicity and convenience. When we consider the reaction of methane to higher hydrocarbons and hydrogen, the absolute value of ΔG^0 (positive or negative) per one mole of methane for methane conversion could be easily estimated by subtracting the $\Delta G_{f/c}^0$ of methane from that of each higher hydrocarbon in Fig. 1 since the value for hydrogen is zero. For example, up to 1300 K, methane has the lowest $\Delta G_{f/c}^0$ among these hydrocarbons, meaning that the conversion to each higher hydrocarbon is not favored thermodynamically. Above 1300 K, benzene has a lower $\Delta G_{f/c}^0$ than that of methane, thus, the conversion of methane to benzene (Table 1,

Table 2 Bond energies in various hydrocarbons (298 K)

C–H bond	E/kJ mol^{-1}	C–C bond	E/kJ mol^{-1}
CH_3–H	434 ± 6	CH_3–CH_3	368 ± 7
C_2H_5–H	412 ± 6	CH_3–C_2H_5	357 ± 8
$(CH_3)_3C$–H	387 ± 8	CH_3–$C(CH_3)_3$	344 ± 9
C_6H_5–H	460 ± 10	CH_3–C_6H_5	417 ± 11

Table 3 ΔG_f^0 of various molecules (298 K)

Molecules	ΔG_f^0/kJ mol^{-1}	Molecules	ΔG_f^0/kJ mol^{-1}
CH_4 (g)	−50.7	H_2O (g)	−228.6
C_2H_2 (g)	209.2	C(s), H_2(g), O_2(g)	0
C_2H_4 (g)	68.2	CO_2 (g)	−394.4
C_2H_6 (g)	−32.8	CO (g)	−137.2
C_3H_6 (g)	62.8	CH_3OH (g)	−162.0
C_3H_8 (g)	−23.5	HCHO (g)	−102.5
C_6H_6 (g)	129.7	NH_3 (g)	−16.5

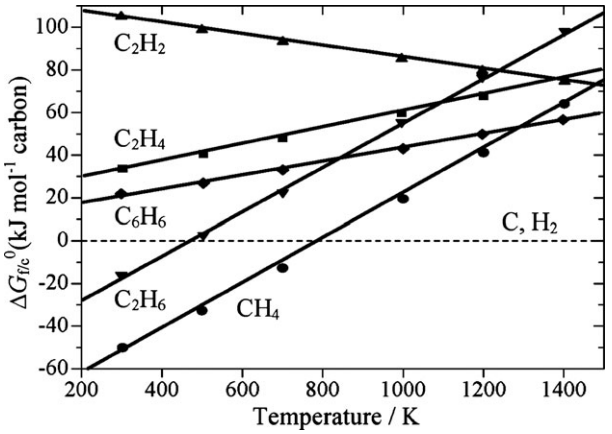

Fig. 1 Gibbs free energy of formation for various hydrocarbons as a function of temperature.

Entry 3) is thermodynamically favorable at this temperature. Fig. 1 also shows that above 800 K, the decomposition of methane to carbon and hydrogen (Table 1, Entry 1) is thermodynamically favored. On the other hand, the plot of $\Delta G^0_{f/c}$ for ethane and methane increase similarly with the temperature. Thus, we can predict that the ΔG^0 for methane conversion to ethane and hydrogen, *i.e.*, NOCM (Table 1, Entry 2), would not be affected by the temperature.

1.3 Developments of methane conversion

1.3.1 Conversion to hydrocarbon. Methane can be converted to higher hydrocarbons with high selectivity *via* NOCM or aromatization (Table 1, Entries 2 and 3). Some catalysts have been reported to show good activity for the reactions. For example, a high C_{2+} yield (37%) was observed on Ru catalyst at 433 K.[4] A high conversion of methane (23%) with high selectivity to benzene (96%) and low amount of coke formation (0.02% of the catalyst weight for 3 h) at 1123 K was achieved on W,Zn/MFI-zeolite catalyst.[5] Since these reactions only proceed at high temperature (see their large ΔG^0 values), the reaction would proceed competitively with the formation of carbon or coke on the catalysts (Table 1, Entry 1). The formation of coke would lead to the fast deactivation of the catalyst.

1.3.2 Oxidation. Research on the oxidation of methane has been performed over a century, and the studies in the early period were already reviewed.[6] The partial oxidation of methane (POM) without a catalyst was recognized by 1903, where hydrogen, carbon monoxide, formaldehyde and formic acid were observed, which could be produced, for example, *via* reactions shown in Table 1, Entries 7 and 8. The formation of methanol in the high-pressure oxidation of methane (5–15 MPa) without a catalyst was first reported in 1932. Since then, many efforts have been made to produce methanol and formaldehyde from methane, by developing the suitable catalysts and reaction conditions.[6,7] For example, the selectivity of methanol as high as 92–96% was achieved on a Cu/SiO_2 catalyst at 573–623 K and high gas pressure (3 Mpa) with a low conversion of methane (6%), while the outstanding yield (22.5%) and selectivity (83%) of formaldehyde was obtained on ironmolybdate at 973 K. Since oxygen is a very reactive molecule, methane can react with molecular oxygen very fast and the consecutive oxidation of products toward the total oxidation can occur easily. Thus, it is very difficult to obtain the desired products with high yield and high selectivity.

Another reaction of methane with oxygen is an oxidative coupling of methane (OCM) to produce higher hydrocarbons, such as ethene and ethane (Table 1, Entry 5), which was reported for the first time in 1982.[8] However, besides ethene (main product) and ethane, CO_2 was also obtained as an undesired by-product, suggesting that the complete oxidation of methane to form CO_2 and H_2O shown in Table 1, Entry 4 could not be avoided. This is because the total oxidation is thermodynamically more favorable than the OCM (see the values of ΔG^0). After intensive efforts for 25 years, no catalyst could be used commercially for the OCM, even though some projects reported a high yield of higher hydrocarbons (C_{2+}) *ca.* 30% and high selectivity more than 80%.[9]

For both POM and OCM, low yield and low selectivity implied the limitations of these systems, which caused the lessening of the researches on the methane conversion *via* oxidation with molecular oxygen. Moreover, the danger of an explosion is also one of the reasons these reactions have not been commercialized yet. However, since methane oxidation could produce heat energy, a recent concept combining oxygen and water in reforming reactions has been developed. This will be described later.

1.3.3 Reforming. Different approaches employing oxidants milder than oxygen, such as carbon dioxide and water, are also being examined and some of them have been put into practice.

The reaction between methane and CO_2 can form syngas (CO and hydrogen). This reaction is called a dry reforming of methane (DRM) or CO_2 reforming of methane as shown in Table 1, Entry 15. The short history about DRM can be found in the literature.[10] DRM is a thermodynamically unfavorable reaction and can only proceed at high temperature, typically more than 1000 K, even by using catalysts. The reaction at high temperature would risk a fast catalyst deactivation as mentioned above. Recently, the performance of the catalyst for the DRM has been improved. For example, Ni–Ce–ZrO_2 catalyst was reported to show excellent methane and CO_2 conversions (97%) and a high resistance for the catalyst deactivation.[11] However, the required reaction temperature was still high (1073 K).

The reaction between methane and water molecules also can produce syngas (CO and hydrogen), which is called steam reforming of methane (SRM), shown in Table 1, Entry 10. The process for this reaction has been commercially established in 1930.[12] A Ni-based catalyst has been reported to show a good activity for SRM. Similar to the case of DRM, since the reaction only occurs at high temperature, the high-energy consumption and the fast catalyst deactivation are the main tasks faced for SRM. For hydrogen production, the SRM process is carried out in two steps in practice. In the first step, the reactions shown in Table 1, Entries 10–12, proceed at high temperatures (*ca.* 1073–1273 K), and in the second step, the reaction shown in Entry 11 is carried out at low temperatures (*ca.* 473–673 K) in order to increase the hydrogen production.

In the first step, an excess amount of H_2O (typically steam/methane ratio is 3) is usually used to reduce the formation of carbon.

A recent concept combining the POM (Table 1, Entry 7) and the SRM (Entry 10) has been applied, *i.e.*, autothermal reforming (ATR) or oxy-steam reforming of methane (OSRM).[13,14] The use of both steam and oxygen can avoid the danger of explosion and reduce the carbon formation in the POM, and can lessen the additional steam cost in the SRM. Since the energy required for endothermic SRM could be obtained from the thermal energy produced by exothermic POM, the overall energy could be reduced. Moreover, the ratio of H_2/CO product could be controlled by the ratio of O_2 and H_2O. For example, a very high methane conversion (99.1%) was reported on the Ni/Ce–ZrO_2 catalyst for OSRM at 1023 K.[13] It is noted that even though a high conversion could be achieved through the reforming reactions mentioned above, methane conversions are always carried out at high temperature.

1.4 Photocatalytic reactions

1.4.1 Properties of photocatalytic reactions. In order to minimize the energy consumption and to reduce the side reactions such as the formation of carbon and coke described above, it is highly desired to lower the reaction temperature. One of the possible alternative ways would be employing photoenergy instead of the thermal energy, *i.e.*, photocatalytic systems would be the potential candidates.

Photocatalytic reactions offer the possibility to promote even difficult reactions at low temperatures, such as room temperature. This would bring some advantages, such as low energy consumption, stability of catalyst (less deactivation), safety and stability of the reactor. The reason why photoenergy could do this great job is because the photoenergy exceeds the activation energy for many kinds of chemical reactions. By Planck constant, we can determine the energy of one photon in a certain wavelength of light. For example, photons of 300 nm wavelength UV light would have energy equal to 399 kJ mol^{-1}. Even though this energy is too low to break directly the H–C bond in methane, it is expected that the use of a suitable photocatalyst would let the methane activation be feasible. Thus, together with the photocatalyst, this high energy of the photon would enable thermodynamically unfavorable reactions ($\Delta G > 0$) to proceed photocatalytically at mild conditions.

In the case of a thermal catalytic reaction, the reaction would be finally affected by the thermodynamic equilibrium. Both the forward and backward reactions usually would proceed even in the equilibrium. On the other hand, it is possible that the photocatalytic reaction is not affected by the thermodynamic equilibrium, although there are some exceptions. In many cases, the forward and backward photocatalytic reaction could be considered as two different reactions which would require different energy for each excitation process and undergo by different mechanisms from each other. Thus, it is possible to decrease or eliminate the undesired backward reaction, meaning that the photocatalytic reaction can break the thermodynamic equilibrium.

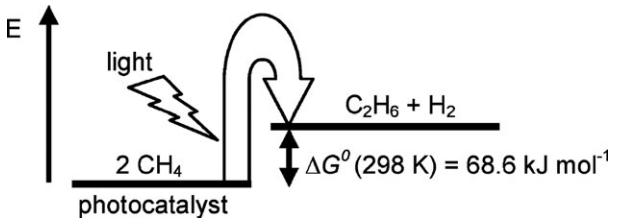

Fig. 2 An example of a photocatalytic system where the photoenergy is converted to the higher chemical potential of products.

There are still many possibilities to explore the undiscovered photocatalytic reactions that are simpler and cleaner without extra consuming of chemicals and energy, or without undesired emissions. In principle, a photocatalyst uses the photoenergy for the activation energy and the increment of the Gibbs free energy (ΔG^0). When the ΔG^0 is positive, the photoenergy is converted to the higher chemical potential of products as shown in Fig. 2. It is very valuable that we can store the photoenergy, which cannot be stored, as chemicals such as hydrogen, which can be stored and transferred easily. It opens the possibility to utilize the abundant solar energy.

All of these matters mentioned above are the benefits of the photocatalytic reactions. However, unfortunately, the yield obtained from the photocatalytic reaction is still very low in many cases. Therefore, development of a photocatalytic system would be highly desired. Since many efforts have been made so far, several studies on the photocatalytic methane conversion could be introduced and discussed in this tutorial review.

1.4.2 The types of heterogeneous photocatalysts. Heterogeneous photocatalysts introduced in this review could be generally divided into two groups: one is the semiconductor photocatalysts and another is the highly dispersed photocatalysts, which are referred to as quantum photocatalysts.[15]

When a 'semiconductor photocatalyst', such as titanium oxide (Fig. 3), absorbs the photoenergy more than its band gap energy, the electron photoexcitation occurs *via* electron transfer from the conduction band (O 2*p*) to the valence band (Ti 3*d*). As a result, many holes and excited electrons are formed on the surface, and then they promote oxidative and reductive reactions, respectively. When this photocatalyst is employed for oxidation of organic compounds with molecular oxygen, non-selective (complete) oxidation would often occur.[15] This type of photocatalyst has a large and intense band

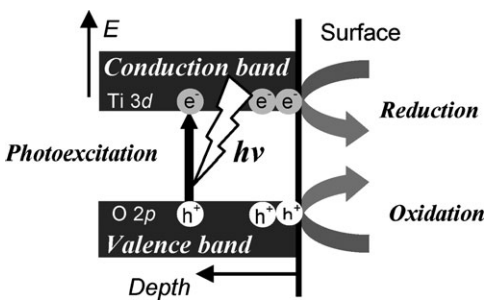

Fig. 3 Photoexcitation of TiO_2 semiconductor photocatalyst and successive photocatalytic reactions.

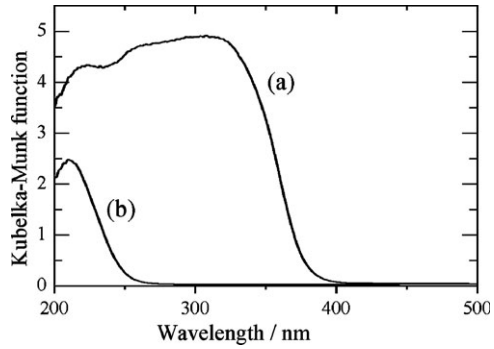

Fig. 4 Diffuse reflectance UV-visible spectra of (a) TiO_2 as a semiconductor photocatalyst and (b) Ti(0.1 mol%)/SiO_2 as a quantum photocatalyst.

in the UV spectrum, implying the ease of the photoexcitation process. As an example, the spectrum of TiO_2 is shown in Fig. 4a.[16]

On the other hand, the photoexcitation process on a 'quantum photocatalyst' would take place at the isolated active sites, for example, highly dispersed titanium oxide on silica (Fig. 5). In this case, the excitation state is localized on a certain moiety in the photoactive species and the number of excited electrons (or holes) is limited to unity on the certain site. When it is applied to oxidation, a rather selective oxidation would occur.[15] Compared to the semiconductor photocatalyst, the quantum photocatalyst would show narrower and less intense absorption bands in UV spectra. As an example, the spectrum of Ti(0.1 mol%)/SiO_2 is shown in Fig. 4b.[16]

2. Photocatalytic conversion of methane

2.1 Methane coupling

Photocatalytic NOCM (Table 1, Entry 2) was first discovered in 1998.[17] This reaction is thermodynamically unfavorable at low reaction temperatures. Thus, it was a surprise to find that this reaction could proceed around room temperature (310 K) over silica, alumina, and silica–alumina photocatalysts under UV irradiation. The reaction test was carried out in a closed quartz reactor (Fig. 6a) for 18 h under UV irradiation from a 250 W Xe lamp. The catalyst was 1 g and only methane (100 μmol) was introduced as the reactant. The products were analysed by gas chromatography (GC). After the 18 h photo-

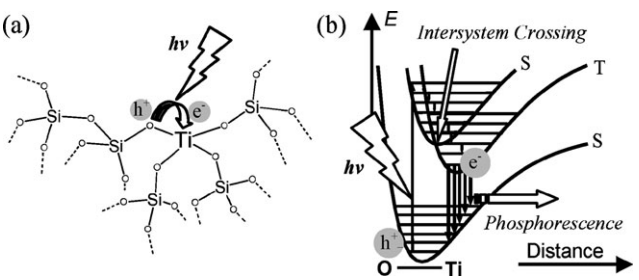

Fig. 5 Photoexcitation of highly dispersed titanium species in a silica matrix as a quantum photocatalyst. (a) A model of the photoactive tetrahedral sites on silica, and (b) a schematic model for photoexcitation localized at Ti–O moiety and phosphorescence emission from the site.

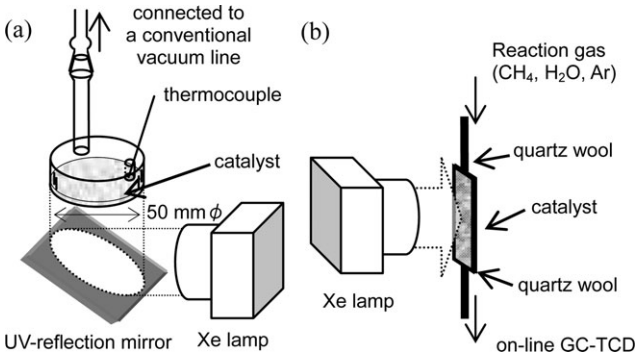

Fig. 6 Schematic drawing of the photoreactor made of quartz. (a) A closed reactor (typically, the bottom was *ca.* 20 cm^2, volume was *ca.* 30–50 cm^3), (b) a flow reactor (typically 10 cm^2 × 1 mm).

reaction, the highest yield of C_2–C_6 products obtained from the methane coupling and the consecutive reactions was achieved on silica–alumina (5.9 C%), where the main product was ethane (60%). No reaction proceeded in the dark or without a photocatalyst. It is worth noting here that the ethane yield on these photocatalysts was much higher than the one calculated from the thermodynamic equilibrium constant (*ca.* 0.0004% at 314 K). Thus, it is confirmed that the photocatalyst selectively promoted the forward reaction, methane activation (probably to form methyl radical), than the reverse reaction, activation of ethane and/or hydrogen, in the photocatalytic NOCM. This would be one of the advantages of the photocatalytic systems.

This great finding was followed by the discoveries of various other photocatalysts promoting the NOCM. We must consider that there are only reductive gases such as methane, ethane and hydrogen as the reactant and the products, in the reactor under photoirradiation. Therefore, the catalyst should work in such non-oxidative/reductive conditions during working as the photocatalyst to promote the reaction. This is one of the important properties required for the photocatalysts in the NOCM.

2.1.1 Quantum photocatalysts. Upon photoirradiation, pure silica materials evacuated at high temperature promoted the NOCM around room temperature.[18] The samples were amorphous silica (554 $m^2\ g^{-1}$) prepared by the sol–gel method and mesoporous silica materials (915 and 994 $m^2\ g^{-1}$). The activities of the mesoporous silica materials were higher than that of the amorphous silica. Some photoabsorption sites were generated through the dehydroxylation of the surface hydroxyl groups by evacuation as a pretreatment at high temperature such as 1073 K. Among them, a kind of surface defect on silica, non-bridging oxygen hole centre (NBOHC, $\equiv$Si–O$^\bullet$) accompanied with E′ centre ($\equiv$Si$^\bullet$), was clarified to be the photoactive sites for the NOCM (eqn (2)). This NBOHC could be excited by 258 nm UV light. The pretreated mesoporous silica had a larger amount of the NBOHC sites than the pretreated amorphous silica.

$$\equiv\text{Si–OH} + \equiv\text{Si–OH} \rightarrow \equiv\text{Si–O}^\bullet + \equiv\text{Si}^\bullet + \text{H}_2\text{O} \quad (2)$$

Although the reaction mechanism has not been clarified, it was suggested that the photoactive sites gave the photoexcitation

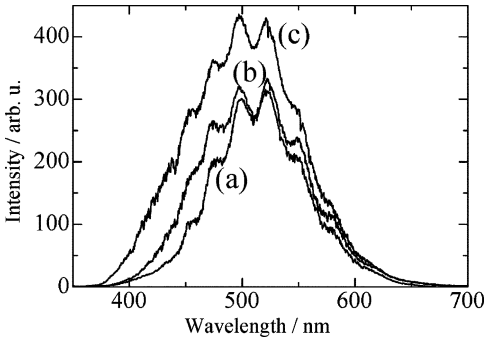

Fig. 7 Photoluminescence spectra of (a) MgO(0.5 mol%)/SiO_2, (b) SiO_2–Al_2O_3(9.1 mol%), and (c) ZrO_2(0.1 mol%)/SiO_2, recorded at 77 K. The excitation wavelength was 300 nm. The samples were pretreated at 1073 K.

energy to the methane molecules through adsorption. Another possibility is that the complex of the active sites and adsorbed methane might be activated by the photoenergy. In either case, the interaction between methane and the photoexcited sites would result in the formation of methyl and hydrogen radicals, which would further react with methane to form ethane and hydrogen.

The activity of amorphous silica was improved when a low loading amount of metal cation such as Al, Mg, and Zr, was introduced to it.[17,19] A fine structure of photoluminescence spectrum was obtained (Fig. 7) only after the sample was treated at high temperature (1073 K). This characteristic fine structure represented the vibrational levels of the excited localized sites (see Fig. 5b), *i.e.*, highly dispersed metal oxide on silica (Si–O–M linkage). Since the properties of the emission sites on these samples such as vibrational levels and lifetime of the excited state and the photocatalytic activity were similar to each other, the photoexcitation process was proposed to occur commonly in the Si–O bond moiety, next to the metal cation (eqn (3)). This would be one of the characteristics of the silica-based quantum photocatalyst.

$$[\text{Si–O–M} \leftrightarrow \text{Si–O}\cdot\cdot\text{M}] \rightarrow [\text{Si}^{+}\text{–O:}]^{*}\cdot\text{M} \qquad (3)$$

In the case of a silica–titania photocatalyst, either prepared by impregnation method or sol–gel method, highly dispersed tetrahedral titanium oxide species, Ti(Td), were found as the main species on the samples with low loadings of Ti such as less than 1 mol%.[16] When the Ti loading increased, the octahedral TiO_2-like nanoparticles were formed. In the photocatalytic methane conversion, only the sample with low loadings exhibited the activity for the NOCM to produce both hydrocarbons and hydrogen. This suggests that the highly dispersed Ti(Td) species were the photoactive sites for the NOCM. On the other hand, the silica–titania with medium and high loadings only produced hydrocarbons without hydrogen formation since the TiO_2 nanoparticles could be reduced by the produced hydrogen during the reaction. With the same amount of Ti loading, silica–titania prepared by the sol–gel method showed higher activity than that prepared by the impregnation method. It was confirmed that the sol–gel method is more effective to form the highly dispersed Ti(Td) species than the impregnation method.

Rare earth oxides are attractive as photoactive materials. However, among the silica-supported rare earth oxides prepared by impregnation method, only silica-supported cerium oxide showed a significant activity for the NOCM.[20] The highly dispersed Ce(III) oxide species that were excited by 265 nm UV light were revealed as the active sites for the NOCM. These active species were mainly obtained when the loading amount of Ce was low, such as 0.1 mol% or less. On the other hand, the samples with high loadings of Ce would have CeO_2 nanoparticles as the main species. The Ce(IV) species would not be the photocatalytic active sites for the NOCM, since Ce(IV) would be reduced by the produced hydrogen upon photoirradiation. Silica-supported cerium oxide showed high activity for the NOCM even though it was evacuated at a lower temperature such as 773 K or room temperature. The active sites should be the highly dispersed Ce(III) oxide species, where the photoexcitation would occur through a kind of *f–d* transition or electron charge transfer from oxygen to Ce(III). The Ce(III) species were also active on alumina support. These support materials played an important role to stabilize cerium species as the highly dispersed Ce(III) species. TiO_2 could not be used as the support, since it was not stable.

2.1.2 Semiconductor photocatalysts. So far, no semiconductor photocatalyst had been found to promote the NOCM producing both ethane and hydrogen. However, recently, it was found that the unsupported Ga_2O_3 showed high activity for the NOCM.[21,22] Different from the case of TiO_2, Ga_2O_3 is unique and attractive since it is not reduced easily and could promote the NOCM. Ga_2O_3 can be excited by UV light of shorter than 290 nm wavelength. The Ga_2O_3 showed higher activity than those of silica-supported gallium oxide samples prepared by the impregnation method, as shown in Fig. 8a.[21] The photoexcitation process of gallium oxide nanoparticles on these silica-supported gallium oxides with high Ga loadings would be similar to that of the unsupported one, *i.e.*, the band-gap photoexcitation of the semiconductor photocatalyst.

On the other hand, it was confirmed that only the sample with low Ga loadings (0.1 mol%) showed the characteristics of the silica-based photocatalysts. The phosphorescence spectrum with the fine structure, like the one in Fig. 7, was observed on this sample. Moreover, this sample showed the

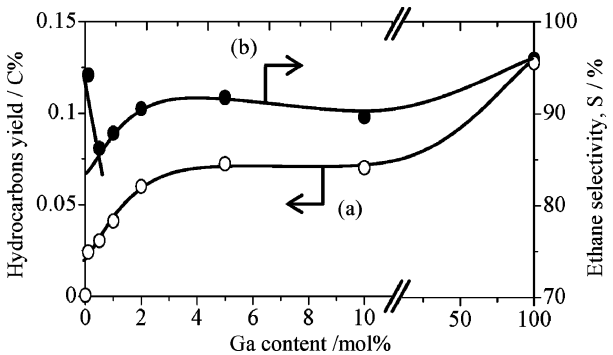

Fig. 8 Dependences of (a) hydrocarbon yield and (b) ethane selectivity on the Ga content of silica-supported gallium oxide samples. 100 shows the Ga_2O_3.

highest ethane selectivity among other silica-supported samples and the plot was out of the lines, as shown in Fig. 8b. It was proposed that the photoexcitation process in this sample would be related to the Si–O moiety.

2.1.3 New design of photocatalyst. Recent development of catalyst preparation method has been successfully achieved to prepare two kinds of active species in one material. Both highly dispersed titanium oxide and cerium oxide on silica were successfully prepared by a two step impregnation method.[23] The order of the metal oxide loading was important; titanium oxide should be loaded first, followed by the cerium oxide loading. The prepared sample showed two absorption bands *ca.* 220 and 265 nm, which were assigned to highly dispersed Ti(Td) species and highly dispersed Ce(III) oxide species on silica, respectively. This photocatalyst showed high activity close to the sum of each activity of the single highly dispersed species. This method successfully increased the amount of the active sites on these quantum photocatalysts for the NOCM.

Besides creating double active sites, a pair of the active sites might also be formed when two kinds of active species were introduced to silica. For example, the SiO_2–Al_2O_3–TiO_2 prepared by sol–gel method exhibited high activity for the photocatalytic NOCM.[24] The active sites proposed were Ti–O–Al sites, where both Al and Ti tetrahedral species formed a pair site. This finding suggests that the ternary oxide systems may provide a synergic effect for the high photocatalytic activity for the NOCM.

For comparison, the activities over various photocatalysts for the NOCM measured in the similar condition are shown in Fig. 9. The main product was ethane in each case. Among them, silica–titania showed the highest yield (0.2%) for the photocatalytic NOCM, followed by the Ga_2O_3 semiconductor photocatalyst that also showed a high activity. Though these conversions were still not enough for the application, they have already exceeded the equilibrium conversion in this condition. During the last decade, we successfully increased the performance of the photocatalyst by a factor of ten. The ternary oxides of quantum photocatalysts would show higher activity than the binary ones (*e.g.* SiO_2–Al_2O_3–TiO_2 showed *ca.* 20 times higher activity than SiO_2–Al_2O_3). Thus, further development can be expected.

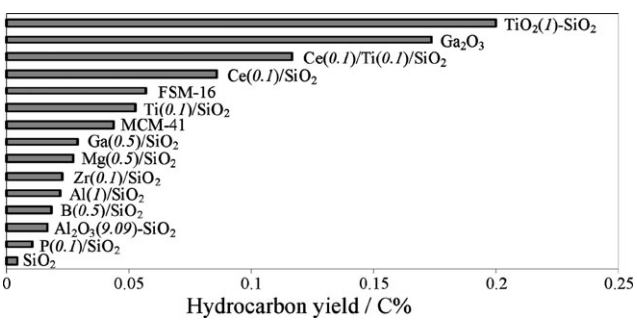

Fig. 9 Activities of various materials for the photocatalytic NOCM, when CH_4 (200 μmol, 7 kPa) and the photocatalyst (0.2 g) were photoirradiated from a 300 W Xe lamp for 3 h around room temperature.

2.2 Methane conversion with O_2

Photocatalytic conversion of methane in the presence of oxygen was reported in 1978 at room temperature under UV irradiation.[25] It was proposed that the hole centres O^- that were produced on the photocatalysts such as TiO_2, V/SiO_2, and P/SiO_2 under UV irradiation ($O^{2-} + h^+ \rightarrow O^-$) would play the important role to attack the methane molecules to produce methyl radicals as the first step.

Similar to the case of thermal catalytic reaction, the complete oxidation of methane to CO_2 and H_2O (Table 1, Entry 4) could not be avoided in the photocatalytic system when using molecular oxygen and a semiconductor photocatalyst, such as TiO_2. It is a challenge for us to convert methane to more useful oxygenated compounds such as methanol, formaldehyde, and carbon monoxide. So far, the photocatalytic methane conversion through partial oxidation of methane (POM) has been the most popular way to obtain the oxygenated compounds. The most intensively studied photocatalysts for the POM are vanadia-based photocatalysts and molybdena-based photocatalysts.

2.2.1 Vanadia-based photocatalysts. V/SiO_2 (V = 2%) produced only a trace amount of ethane and formaldehyde at room temperature under UV irradiation in the photocatalytic POM.[25] The major product was CO_2. Further research successfully improved the activity and the selectivity of vanadia-based photocatalysts for the POM by employing mild thermal energy together with the photoenergy. For example, when the photocatalytic reaction was carried out at 493 K in a flow reactor, formaldehyde was obtained with 76 mol% selectivity and 0.48 mol% one-pass yield on V_2O_5/SiO_2 (0.6 mol% V).[26] Both UV irradiation and a reaction temperature as high as 500 K were essential. The addition of water was found to inhibit the reaction. Our group tested the activity of V/SiO_2 for the POM under UV irradiation at 493 K.[27] It was confirmed that the high photoactivity for formaldehyde formation (1.8–2.6% yield) with high selectivity (80–92%) was obtained when the loading amount of V was very low, *ca.* 0.01–0.1 mol%. When the loading amount of V increased, the total oxidation to CO_x proceeded more easily, resulting in a lower activity and selectivity to formaldehyde. In the photoreaction at higher temperature (>673 K), both the conversion of methane and the selectivity to formaldehyde decreased, which would be due to the reduced lifetime of the photoexcitation state and the increase of the thermally catalysed consecutive oxidation of formaldehyde to CO_2, respectively.

A large specific surface area seems to be an important factor contributing the high activity of vanadia-based photocatalysts. Under UV irradiation at 493 K, with the same amount of V loading, a mesoporous silica-supported photocatalyst was reported to show much higher activity to produce formaldehyde than the amorphous silica-supported version.[28] The yield and selectivity of formaldehyde product were *ca.* 0.3% and 95.4%, respectively. In all cases mentioned above, the four-coordinated species having V=O bond on the surface (highly dispersed and isolated vanadium oxide surface species) were proposed to be the active sites for selective formation of formaldehyde. The high surface area of the support would

favor the high dispersion of the vanadium oxide species resulting in both a high photocatalytic activity and a high selectivity for the formaldehyde formation.

2.2.2 Molybdena-based photocatalysts. Although TiO_2 and MoO_3 photocatalysts only produced CO_2, TiO_2-supported MoO_3 produced both CO and CO_2 in an almost equal amount in a closed reactor under UV irradiation around room temperature.[29] The activity of TiO_2-supported MoO_3 is much higher than that of either TiO_2 or MoO_3, suggesting the synergic interaction between TiO_2 and MoO_3. The photoexcited electrons and holes would migrate through the conjugation between them, which would assist the local separation and prevent their recombination, and thus, would give a high activity.

Photocatalytic POM to methanol was reported on a MoO_3/SiO_2 catalyst.[30] The reaction was carried out in a circulated closed system. A low yield of methanol was detected under UV irradiation at 313 K without any CO_x molecule formation. However, MoO_3/SiO_2 was turned to blue after photoirradiation for a long time, suggesting the reduction of MoO_3. When the photoreaction was carried out at a higher temperature (373 K), the color of the catalyst did not change, suggesting that the facile oxidation of the reduced sites by oxygen occurred at this temperature. Elevated temperature also promoted desorption of methanol. Therefore, this synergic effect of photoenergy and mild thermal energy promoted the reaction with less deactivation. The addition of Cu^{2+} to the MoO_3/SiO_2 catalyst also enhanced the methanol formation, from 2 μmol h^{-1} to 6 μmol h^{-1}. It was proposed that the increase of the formation rate under UV irradiation was possibly caused by the longer lifetime of the active O^- centres photoformed by the charge transfer from O 2*p* to the valence *d* orbital of Cu^{2+}. In addition, silica-supported $CuMoO_4$ exhibited absorption in the visible region and gave a high methanol formation (2.8 μmol h^{-1}) under visible irradiation.

In a flow reactor, the MoO_3/SiO_2 (Mo = 4.4 wt%) exhibited photocatalytic activity for methane oxidation to formaldehyde and methanol, with the yields of 0.08% and 0.03%, respectively, without any CO_x formations at 493 K.[31] It was suggested that the active sites were the coordinatively unsaturated Mo═O species in the terminal position of less dispersed molybdenum species on silica, but not on the large crystallites of MoO_3.

So far, it is still difficult to obtain both high activity and high selectivity for the photocatalytic POM by using molecular oxygen. This is because of the high reactivity of the oxidant. In many cases, the addition of mild thermal energy seemed to be effective in promoting the photocatalytic reaction, which may be applicable for other photocatalytic systems.

2.3 Methane conversion with H_2O

Other oxidants milder than molecular oxygen have also been examined in photocatalytic conversion of methane to obtain some organic products and/or hydrogen. Here, the photocatalytic methane conversion by using water molecules as the oxidant will be introduced.

2.3.1 Photocatalytic methanol formation. Photocatalytic conversion of methane to methanol by using water as the oxidant (Table 1, Entry 9) was reported to occur on WO_3 doped with lanthanum under either UV or visible irradiation at 343 K.[32] In a high pressure reactor, the catalyst was suspended in water (*ca.* 750 mL) containing methyl viologen dichloride as an electron-transfer agent by mechanical stirring. A mixture of methane (5 mL min^{-1}) and helium (16 mL min^{-1}) was then introduced to the reactor. The products were analysed online by a quadrupole mass spectrometer. Methane conversion was *ca.* 4% and the main products were hydrogen and methanol at 1 MPa. The observed side products were ethane, oxygen, formic acid, and CO_2. The conversion depended on the dissolved methane concentration in water. The reaction occurred only above 343 K at atmospheric pressure (0.1 MPa), but it occurred at a lower temperature (323 K) at 10 MPa. The addition of hydrogen peroxide increased the conversion of methane. It was proposed that the hydroxyl radical would react with methane to give a methyl radical, which would further react with the additional water to produce methanol and hydrogen. An experiment for the conversion of methane hydrate was also carried out similarly. It was found that photocatalytic conversion of methane hydrate could occur even at low temperatures such as 258 K. In this reaction, methanol and hydrogen were also obtained as the major products.

Conversion of methane to methanol by using a visible laser (514 nm) and a WO_3 catalyst was reported to occur at room temperature.[33] The reaction was carried out in a batch reactor, in which the catalyst was suspended in water with stirring in the flow of methane. The products observed were methanol, O_2, and CO_2. The maximum yield of methanol was *ca.* 32 mg dm^{-3} when the laser power was 1.5 W and the catalyst amount was 0.3 g. The addition of H_2O_2 has no effect in enhancing the methanol yield, but the addition of an electron capture agent like Fe^{3+} could optimize the yield. Here Fe^{3+} would inhibit the generation of O_2^- and CO_2 by capturing the conduction band electron to produce Fe^{2+}. This keeps the concentration of methanol and oxygen constant over a prolonged period.

2.3.2 Photocatalytic SRM. Recently, it was found that a Pt/TiO_2 photocatalyst promoted the photocatalytic SRM (Table 1, Entry 12) around room temperature,[34,35] corresponding that both the SRM and the consecutive water–gas shift reaction (Table 1, Entries 10 and 11) occurred simultaneously. The photocatalytic reaction tests were carried out with a fixed-bed flow photoreactor (Fig. 6b). The photocatalyst (0.5 g) was used around 323 K at atmospheric pressure upon photoirradiation from a 300 W Xe lamp in a flow of the mixed gases (CH_4, H_2O and Ar). High activity was obtained on Pt/TiO_2 photocatalysts having large surface area of anatase TiO_2 and enough loading amount (>0.1 wt%) of metallic Pt nanoparticles. H_2 and CO_2 were observed as the main products upon photoirradiation, as shown in Fig. 10. Trace amounts of C_2H_6 and CO were observed as minor products. After an induction period, the molar ratio of H_2 to CO_2 in the outlet gas became close to four (Fig. 10c), confirming that the photocatalytic SRM proceeded as the main reaction. The photocatalytic NOCM would also be promoted to produce

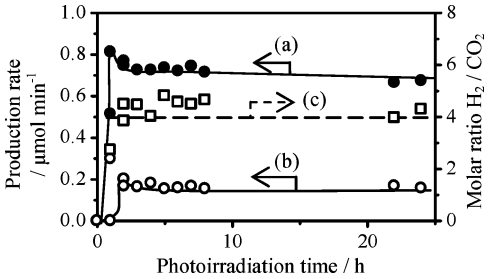

Fig. 10 Time course of the production rate for (a) H_2 and (b) CO_2, and that of (c) the molar ratio of H_2 to CO_2 over Pt(0.1)/TiO_2 in the flow of CH_4 (50%) and H_2O (1.4%). Total flow rate was 50 mL min^{-1}.

C_2H_6 and H_2 as the side reaction. When the H_2 production rate was 0.7 μmol min^{-1}, the methane conversion was calculated to be 0.02%, and the reaction selectivity for the photocatalytic SRM was 85%, in this condition. In this system, H_2O and CH_4 would be activated to form the surface reaction intermediates, $[CH_2O]_n$. The intermediates react with H_2O to complete the reaction scheme (Table 1, Entry 12). In addition, it is unique that the surface intermediates accelerated the reaction, which would be due to their hydrophobic property.

Platinum-loaded lanthanum-doped sodium tantalate, Pt/$NaTaO_3$:La was found to show higher activity for the photocatalytic SRM than the other catalysts, such as Pt/TiO_2, $NaTaO_3$:La and Ni-loaded $NaTaO_3$:La.[35] By-products were hardly observed in this case. The H_2 production rate became constant (1.5 μmol min^{-1}) after the very short induction period and it sustained without deactivation for a long period, over 18 h. The molar ratio of H_2 to CO_2 in the outlet gas was almost constant to be four in the steady state. The turnover frequency per surface Pt atom was estimated to be 68 h^{-1}. High crystallinity of the $NaTaO_3$:La semiconductor and the suitable loading amount of Pt were found to be important for obtaining the high activity in the photocatalytic SRM. In this system, the highest H_2 production rate observed was 4.5 μmol min^{-1} (6.6 mL h^{-1}), corresponding to 0.6% methane conversion, over Pt(0.03 wt%)/$NaTaO_3$:La upon photoirradiation of maximum intensity (116 mW cm^{-2}) from the Xe lamp in the flow of a mixture of 1% H_2O and 10% CH_4 (total flow rate was 50 mL min^{-1}). In this condition, the methane conversion (0.6%) clearly exceeded the equilibrium yield (0.2%), which would be one of the advantages of the photocatalytic reaction system. This fact suggests that the photocatalyst could activate CH_4 and H_2O to form the surface intermediates and products (forward reaction) but it could not promote the reverse reaction for each step, *i.e.*, the formation of intermediates from H_2 and CO_2 or the formation of CH_4 and H_2O from the intermediates.

The apparent quantum yield in the wavelength range of 240–270 nm on Pt(0.05 wt%)/$NaTaO_3$:La was estimated to be 30% under the low intensity light (2 mW cm^{-2}). It was clarified that the present photocatalytic SRM could produce H_2 more efficiently than the photocatalytic water splitting systems. Although the possibility of the reverse reaction is one of the problems with the photocatalytic water splitting, the reverse reaction seems to be difficult to proceed in the photocatalytic SRM (Table 1, Entry 12). In addition, the ΔG^0 of this SRM is lower than that of the water splitting (ΔG^0(298 K) = 237 kJ mol^{-1} for liquid water). These would also be advantages of the photocatalytic SRM.

This photocatalytic SRM system can produce H_2 from renewable resources (biomethane and water) and natural energy (photoenergy such as solar energy). At present, Pt/$NaTaO_3$:La shows the highest activity in the photocatalytic SRM.

2.4 Methane conversion with CO_2

As a weak oxidant, CO_2 might be a good candidate to replace the reactive oxygen molecule. Its role as a greenhouse gas has motivated many efforts not only to reduce its emission but also to utilize and convert it to more useful compounds. However, CO_2 is a very stable molecule (more stable than methane) and it is difficult to activate it. Several studies on the photocatalytic reaction between methane and CO_2 have been carried out and some of them will be introduced here.

In order to reduce CO_2 to CO with methane, the photocatalytic reaction between methane and CO_2 was examined over MgO and ZrO_2 at room temperature.[36] After the photoreaction, CO and hydrogen were detected, although the amount of hydrogen was very low compared to the amount of produced CO. It was confirmed that CO was produced from CO_2, not from CH_4. Methane took part in the formation of surface acetate and formate. One of the reactions could be described as shown in Table 1, Entry 13. It was proposed that CO would be produced from the reaction between the activated CO_2 and the surface formate under irradiation.

Photocatalytic conversion of methane and CO_2 to produce acetone as the major product with high selectivity was reported to proceed on Cu/CdS-TiO_2/SiO_2 under UV irradiation at 393 K (Table 1, Entry 14).[37] The selectivity for acetone was 92.3% at 1.47% conversion of methane and 0.74% conversion of CO_2. Other products such as ethane and CO were also detected with selectivities 3.1% and 4.6%, respectively. At lower temperature (353 K) only ethane and CO were produced with selectivities 46.7% and 53.3%, respectively. Unfortunately, the conversion of methane and CO_2 reduced to zero in about 2 h due to the photocorrosion of CdS by TiO_2.

Recently, photocatalytic conversion of both methane and CO_2 to produce both CO and hydrogen, *i.e.*, photocatalytic DRM (Table 1, Entry 15) was reported to proceed on Ga_2O_3 under UV irradiation at 473 K in a closed reactor (Fig. 6a).[22] Besides DRM, photocatalytic NOCM also proceeded as the side reaction. Therefore, CO, hydrogen, and hydrocarbons (mainly ethane) were obtained as the products. At room temperature only a trace amount of CO was obtained, indicating that the mild thermal energy is required for the photocatalytic DRM to proceed. The CO product was found to increase with the reaction temperature (Fig. 11a). The activation energy (E_a) for CO formation was roughly estimated to be *ca.* 10 kJ mol^{-1} at 473–673 K and *ca.* 60 kJ mol^{-1} at 673–873 K. These E_a values obtained here were much lower than that obtained from the catalytic thermal DRM on this Ga_2O_3 sample without UV irradiation (E_a = 110 kJ mol^{-1} at 773–973 K). It was proposed that the mild thermal energy at 473–673 K was used for a mild activation step such as product desorption process or electron migration from the bulk to the

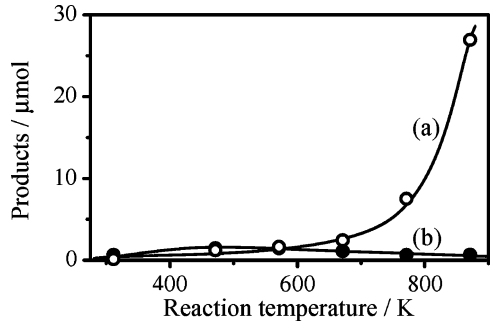

Fig. 11 Dependences of (a) CO and (b) hydrocarbon products on the temperature of the photocatalytic reaction between CH_4 and CO_2 (200 μmol each) over Ga_2O_3 (0.2 g) for 3 h.

surface of Ga_2O_3 and the photoenergy mainly promoted the DRM. At a higher reaction temperature (673–873 K), CO would be formed mainly *via* photocatalytic DRM even though thermal catalytic reactions also partially contributed for the CO formation. The methane conversion at 473 K was 0.27% in the DRM after 3 h, which was superior to the equilibrium conversion (0.21%). This fact means that photocatalysis is a potential technology to promote the difficult reaction at milder reaction conditions beyond the thermodynamic equilibrium conversion.

2.5 Methane conversion with aqueous ammonia

Photoirradiation of aqueous 2 M NH_4Cl or NH_3 (*ca.* 28%) deaerated solution under slow continuous bubbling of methane in the presence of a Pt/TiO_2 photocatalyst for more than 60 h produced a mixture of amino acids although the total yield of amino acids was less than 0.5 μmol.[38] The products were glycine, alanine, serine, aspartic acid, and glutamic acid. For example, one of the reactions can be described as shown in Table 1, Entry 16. This result is very interesting in considering the initial stage of chemical evolution and prebiological synthesis of organic compounds from simple components. This reaction also provides some possibilities for the development of new chemical synthesis methods from methane.

3. Conclusions and outlooks

As mentioned above, methane can be converted in various ways. Especially in this tutorial review, we introduced some photocatalytic reaction systems for the methane conversion, *i.e.*, the direct methane conversion to hydrocarbons (NOCM), the partial oxidation (POM), the steam reforming (SRM), the dry reforming (DRM) and others. These photocatalytic reaction systems provide us with many possibilities to activate methane.

As mentioned above, photocatalysis has some advantages. In some photocatalytic systems, the reaction could proceed beyond the thermodynamic barrier to give selected products under mild conditions. The low temperature process would be beneficial for some reasons. Since other molecules used to reduce the activation energy would not be required, newly designed photocatalytic reaction systems might become a simple and clean system without consumption of extra energy and chemicals, and without undesirable emissions. It is also important that the photocatalysis can convert the solar energy to chemical compounds having high potential such as hydrogen, which can be stored.

However, most of the reported photocatalytic methane conversions give a low product yield and a low energy efficiency, which are still very far from our demands. Thus, while we must further develop the performance of these photocatalytic systems, we must consider the place where the photocatalytic reaction systems can be applied efficiently. For example, biomethane gently produced through biotechnology might be converted to hydrogen by the photocatalytic SRM, DRM or the combination of these reactions. We might utilize the abundant methane hydrate directly *via* photocatalytic SRM since methane hydrate is the source of both methane and water, and the photocatalytic SRM could proceed at low temperature. Besides the development of photocatalysts, other technologies should also be developed for actual use, such as efficient light sources, design of photocatalytic reactor, and gas separation.

The photocatalytic conversion of methane has not been popularly studied to date. There should still be many undiscovered photocatalysts and photocatalytic systems. Even the known photocatalytic systems have enough potential to be much improved. It is expected that further development would bring the photocatalytic system for methane conversion closer to being a real application.

Acknowledgements

We thank warmly all the co-workers who have contributed to our own works in this area. This work was partially supported by a Grant-in-Aid for Scientific Research on Priority Areas (No. 19028023, "Chemistry of Concerto Catalysis") from the Ministry of Education, Culture, Sports, Science and Technology (MEXT) of the Japanese Government (H.Y.).

References

1. P. Forster, V. Ramaswamy, P. Artaxo, T. Berntsen, R. Betts, D. W. Fahey, J. Haywood, J. Lean, D. C. Lowe, G. Myhre, J. Nganga, R. Prinn, G. Raga, M. Schulz and R. Van Dorland, in *Climate Change 2007: The Physical Science Basis. Contribution of Working Group I to the Forth Assessment Report of the Intergovernmental Panel on Climate Change*, ed. S. Solomon, D. Qin, M. Manning, Z. Chen, M. Marquis, K. B. Averyt, M. Tignor and H. L. Miller, Cambridge University Press, Cambridge, United Kingdom and New York, NY, USA, 2007, pp. 129–234.
2. P. A. Cook, M. N. R. Ashfold, Y.-J. Lee, K.-H. Jung, S. Harich and X. Yang, *Phys. Chem. Chem. Phys.*, 2001, **3**, 1848, and references therein.
3. T. V. Choudhary, E. Aksoylu and D. W. Goodman, *Catal. Rev. Sci. Eng.*, 2003, **45**, 151 and references therein.
4. M. Belgued, H. Amariglio, P. Pareja, A. Amariglio and J. Saint-Just, *Catal. Today*, 1992, **13**, 437.
5. J.-L. Zeng, Z.-T. Xiong, H.-B. Zhang, G.-D. Lin and K. R. Tsai, *Catal. Lett.*, 1998, **53**, 119.
6. H. D. Gesser, N. R. Hunter and C. B. Prakash, *Chem. Rev.*, 1985, **85**, 235 and references therein.
7. M. J. Brown and N. D. Parkyns, *Catal. Today*, 1991, **8**, 305, and references therein.
8. G. E. Keller and M. M. Bhasin, *J. Catal.*, 1982, **73**, 9.
9. Y. S. Su, J. Y. Ying and W. H. Green, Jr, *J. Catal.*, 2003, **218**, 321, and references therein.

10. Y. H. Hu and E. Ruckenstein, *Catal. Rev. Sci. Eng*., 2002, **44**, 423, and references therein.
11. H.-S. Roh, H. S. Potdar and K.-W. Jun, *Catal. Today*, 2004, **93–95**, 39.
12. R. T. Haslam and R. P. Russell, *Ind. Eng. Chem*., 1930, **22**, 1030.
13. H.-S. Roh, K.-W. Jun, W.-S. Dong, S.-E. Park and Y.-S. Baek, *Catal. Lett*., 2001, **74**, 31.
14. J. R. Rostrup-Nielsen, *Catal. Today*, 1994, **21**, 257.
15. H. Yoshida, *Curr. Opin. Solid State Mater. Sci*., 2003, **7**, 435, and references therein.
16. L. Yuliati, H. Itoh and H. Yoshida, *Stud. Surf. Sci. Catal*., 2007, **172**, 457.
17. Y. Kato, H. Yoshida and T. Hattori, *Chem. Commun*., 1998, 2389.
18. L. Yuliati, M. Tsubota, A. Satsuma, H. Itoh and H. Yoshida, *J. Catal*., 2006, **238**, 214.
19. L. Yuliati, T. Hattori and H. Yoshida, *Phys. Chem. Chem. Phys*., 2005, **7**, 195, and references therein.
20. L. Yuliati, T. Hamajima, T. Hattori and H. Yoshida, *J. Phys. Chem. C*, 2008, **112**, 7223.
21. L. Yuliati, T. Hattori, H. Itoh and H. Yoshida, *J. Catal*., DOI: 10.1016/j.jcat.2008.05.022.
22. L. Yuliati, H. Itoh and H. Yoshida, *Chem. Phys. Lett*., 2008, **452**, 178.
23. L. Yuliati, H. Itoh and H. Yoshida, *Chem. Lett*., 2006, **35**, 932.
24. H. Yoshida, N. Matsuhita, Y. Kato and T. Hattori, *J. Phys. Chem. B*, 2003, **107**, 8355.
25. S. L. Kaliaguine, B. N. Shelimov and V. B. Kazansky, *J. Catal*., 1978, **55**, 384.
26. K. Wada, H. Yamada, Y. Watanabe and T. Mitsudo, *J. Chem. Soc., Faraday Trans*., 1998, **94**, 1771.
27. H. Yoshida, T. Sunada and T. Hattori, unpublished work.
28. H. H. López and A. Martínez, *Catal. Lett*., 2002, **83**, 37.
29. K. R. Thampi, J. Kiwi and M. Grätzel, *Catal. Lett*., 1988, **1**, 109.
30. M. D. Ward, J. F. Brazdil, S. P. Mehandru and A. B. Anderson, *J. Phys. Chem*., 1987, **91**, 6515.
31. K. Wada, K. Yoshida and Y. Watanabe, *J. Chem. Soc., Faraday Trans*., 1995, **91**, 1647.
32. C. E. Taylor, *Catal. Today*, 2003, **84**, 9.
33. M. A. Gondal, A. Hameed and A. Suwaiyan, *Appl. Catal., A*, 2003, **243**, 165.
34. H. Yoshida, K. Hirao, J. Nishimoto, K. Shimura, S. Kato, H. Itoh and T. Hattori, *J. Phys. Chem. C*, 2008, **112**, 5542.
35. H. Yoshida, S. Kato, K. Hirao, J. Nishimoto and T. Hattori, *Chem. Lett*., 2007, **36**, 430.
36. K. Teramura, T. Tanaka, H. Ishikawa, Y. Kohno and T. Funabiki, *J. Phys. Chem. B*, 2004, **108**, 346, and references therein.
37. D. Shi, Y. Feng and S. Zhong, *Catal. Today*, 2004, **98**, 505.
38. H. Reiche and A. J. Bard, *J. Am. Chem. Soc*., 1979, **101**, 3127.

